Icarus 358 (2021) 114172

Contents lists available at ScienceDirect

Icarus

journal homepage: www.elsevier.com/locate/icarus

The precession constant and its long-term variation

ARTICLE INFO

Keywords
Precession constant
Dynamical flattening
Mantle convection
Glacial isostatic adjustment
Climate change
Earth rotation

ABSTRACT

The dynamical flattening of the Earth, H, related to the precession constant, is a fundamental astro-geodetic parameter that appears in studies of the Earth's rotation and orbital evolution. We present numerical predictions and observations of the variation in H over time scales ranging from tens of millions of years to decades. The geophysical processes controlling this variation include solid-state convection in the rocky mantle of the Earth that drives plate tectonics, isostatic adjustments due to ice age loading, and ice-ocean mass transfer linked to modern global climate change. The time dependence of H is complex and non-linear, and thus, in contrast to previous suggestions, cannot be captured by a constant rate parameter.

1. Introduction

The dynamic flattening of the Earth, H, is a measure of the difference between the polar moment of inertia (C) and the mean of the equatorial moments of inertia (A, B) of the planet:

$$H = \frac{1}{C}\left[C - \frac{1}{2}(A+B)\right] \quad (1)$$

H is a fundamental parameter in precession and nutation theories of the Earth, as well as a series of other rotational normal modes of widely varying frequency (e.g. Wahr, 1981; Dehant and Capitaine, 1996; Chao, 2017). Dynamic flattening also plays an important role in a range of global geophysical studies – either explicitly or implicitly – through its connection to changes in the planetary spin rate (or, alternatively, "length-of-day" in geodesy) or dynamical form factor, J_2. For example: (1) satellite-based estimates of the secular rate of change of J_2 after ~1990 are thought to be impacted by the onset of significant polar ice sheet melting (Cox and Chao, 2002); (2) variations in J_2 associated with ongoing, residual effects of the last ice age, as well as with tidal dissipation and other factors, combine to explain the slowing of the Earth's rotation rate over the past three millennia that has been estimated from ancient eclipse observations (Stephenson and Morrison, 1984, 1995; Stephenson, 2003; Mitrovica et al., 2015); (3) perturbations in the dynamical flattening driven by mass changes arising from ice age effects and solid-state convective mantle flow alter Milankovitch (precession, obliquity) band variations in climate proxy records (Laskar et al., 1993; Forte and Mitrovica, 1997; Mitrovica et al., 1997; Pälike and Shackleton, 2000; Lourens et al., 2001; Morrow et al., 2012); and (4) geological measurements of the period of Earth's rotation during the Proterozoic Eon (~ 620 Ma) that are based on tidal rhythmites reflect long-term tidal braking and dissipation in the Earth-Moon-Sun system (Williams, 1997), which would also be manifest as a trend in H.

The above discussion raises the question: Is the rate of change of dynamical flattening constant and, if not, what is the temporal structure of its variability? Burša et al. (2008) estimated that the long-term variation in $dH/dt = -8.45 \times 10^{-11}\ \mathrm{yr}^{-1}$ from satellite data over the period 1979–2002 (Cox and Chao, 2002). They argue that this rate should be treated as a fundamental astro-geodetic parameter and suggest that the trend may remain valid for the past 650 Myr; this argument is based on the fact that the current rate of tidal braking of the Earth's rotation rate would, if applied over this long time period, lead to a rotation period at 650 Ma (henceforth "Ma" denotes "million years ago") relatively close to the geological inference of ~21.8 h. Putting aside geophysical modeling of variations in H, there are a variety of reasons to be sceptical of this argument. First, as noted above, the trend in the dynamical form factor, or dJ_2/dt, has varied significantly across the satellite period. For example, Roy and Peltier (2011) estimate rates of $-3.7 \times 10^{-11}\ \mathrm{yr}^{-1}$ for the period 1976–1992 and $-0.9 \times 10^{-11}\ \mathrm{yr}^{-1}$ for 1992–2009 (equivalent values for dH/dt are $-11.1 \times 10^{-11}\ \mathrm{yr}^{-1}$ and $-2.7 \times 10^{-11}\ \mathrm{yr}^{-1}$, respectively). The estimate of $dH/dt = -8.45 \times 10^{-11}\ \mathrm{yr}^{-1}$ in Burša et al. (2008), based on the results of Cox and Chao (2002), is thus a time-weighted average of these two values. Second, ongoing isostatic adjustment in response to ice age loading over the last few million years dominates the pre-1992 variation in H, and thus any trend in the precession constant over this period cannot be constant, but will instead reflect the time scales of ice age cyclicity. Third, the current dynamic flattening of the Earth is known to exceed the form of a rotating planet in hydrostatic equilibrium by ~ 1% (Nakiboglu, 1982; Chambat et al., 2010). This excess flattening is driven by convective flow in the mantle and will thus vary over the timescale associated with that process, which is tens of millions of years. Finally, the present rate of tidal braking of the Earth's rotation must be anomalously high, because a back-projection of that rate leads to the so-called "time-scale problem" of Lunar origin (i.e., the Moon's orbital radii would place it at the Roche limit only ~2 billion years ago; Kaula and Harris, 1975). The likely resolution of this problem is that ocean tidal dissipation would have been lower during the time of the Pangean supercontinent (~340–170 Ma), and during previous supercontinent periods, with a consequent reduction in rates of change of both H and Earth's rotation period during these times (Hansen, 1982).

In this article, we describe new predictions of the variation in the dynamical ellipticity over time scales ranging from tens of millions of years to centuries, based on geophysical modeling of changes in Earth's

https://doi.org/10.1016/j.icarus.2020.114172
Received 15 March 2020; Received in revised form 30 August 2020; Accepted 6 October 2020
Available online 21 October 2020

shape associated with mantle convective flow over the past 50 million years and ice mass flux across the Plio-Pleistocene glacial cycles (i.e., the past 3 Myr). We also map a recent, satellite-derived time series of J_2 into a variation in H from 1976 to 2012. The predictions, together with the satellite derived time series, provide a measure of the natural — and human-induced — variability in Earth's dynamical flattening. This variability is complex, and it cannot be captured by a constant rate term.

2. Mathematical background

Perturbing Eq. (1), and using the fact that the trace of the inertia tensor is invariant during non-uniform deformation (e.g. Rochester and Smylie, 1974), i.e.,

$$\delta A + \delta B + \delta C = 0, \tag{2}$$

yields the following expression for the variation in H

$$\delta H = \left[\frac{3}{2} - H\right]\frac{\delta C}{C}. \tag{3}$$

(NB. we comment in Section 3 on the impact of uniform deformation on these equations). Since $H \sim 0.00327$, this expression can be approximated as

$$\delta H \approx \frac{3}{2}\frac{\delta C}{C}. \tag{4}$$

The dynamical form factor, J_2, is defined as

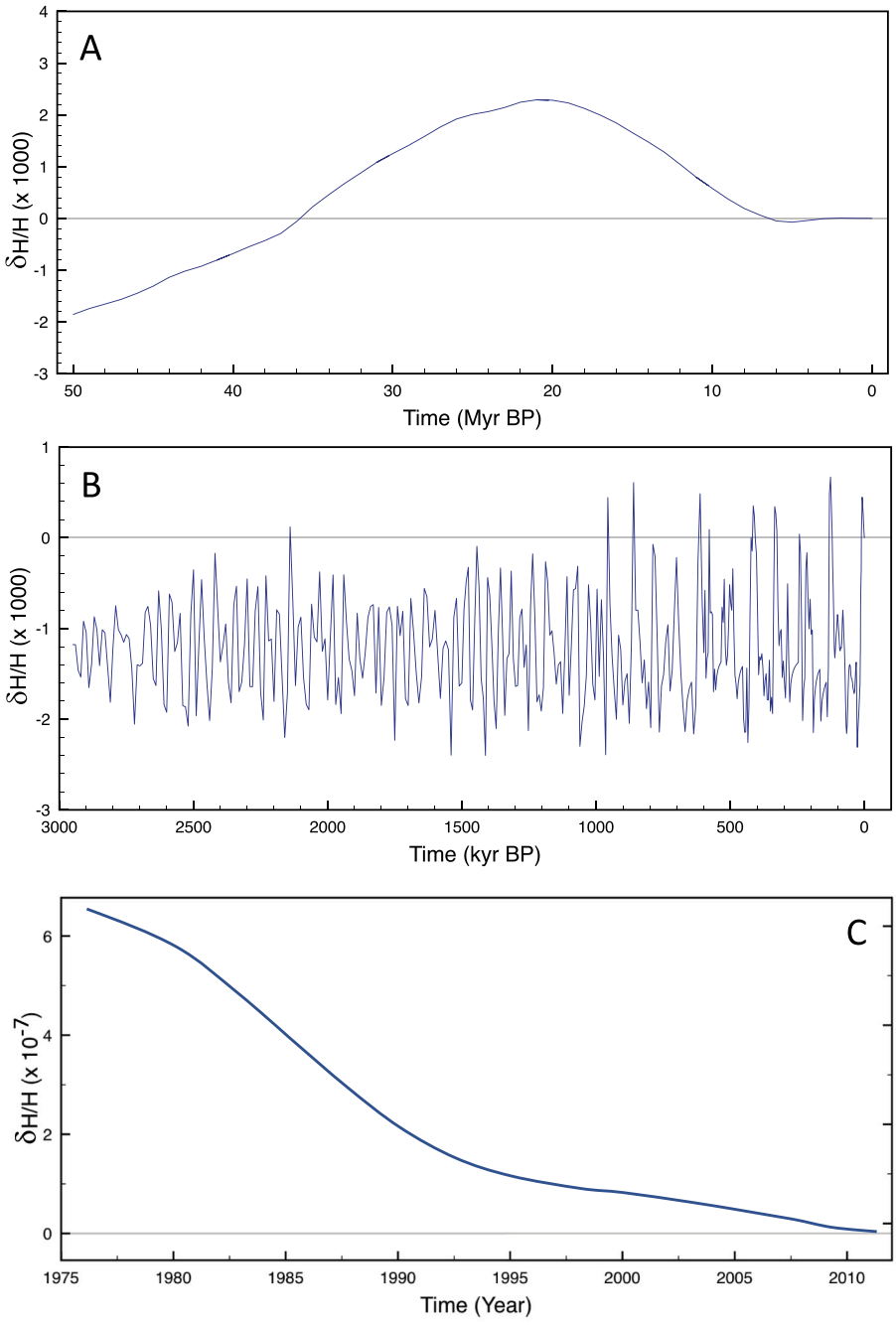

Fig. 1. (A) Relative perturbation in the dynamic flattening of the Earth predicted using the adjoint reconstruction of mantle convective flow over the past 50 Myr (see text). (B) As in (A), except for a reconstruction of changes in the dynamic flattening since 3 Ma predicted from a simulation of ice age dynamics alone (see text). The numerical predictions in frames (A) and (B) are both based on a common model of the Earth's radial viscosity profile that was derived by simultaneously inverting a large suite of global geophysical data related to mantle convection and ice age dynamics (Mitrovica and Forte, 2004; see text). (C) Time series of the relative perturbation in the dynamic flattening estimated from satellite altimetry records since 1975. The time series is computed from the results of Cheng et al. (2013). All results are plotted relative to the present day value, or in the case of frame (C), 2012.

$$J_2 = \frac{1}{M_e a^2}\left[C - \frac{1}{2}(A+B)\right], \tag{5}$$

where M_e and a are the mass and radius of the Earth, respectively. Combining eqs. (1) and (5) yields the following relationship

$$H = \frac{M_e a^2}{C} J_2. \tag{6}$$

Taking the first variation of this expression, and once again using the fact that $H << 1$, yields

$$\delta H = \frac{M_e a^2}{C}\delta J_2. \tag{7}$$

Since $C \tilde{} \frac{1}{3} M_e a^2$, the scaling factor on the right-hand side of Eq. (7) is ~3. This simple relationship was applied to relate expressions for dJ_2/dt and dH/dt that were used in Section 1.

In the results below, we will consider predictions and observations of the relative perturbation in the dynamic flattening, $\delta H/H_0$, where H_0 is the present-day value (0.003274) and the perturbation δ is defined relative to this value (Fig. 1). As a guide to interpreting the impact of such signals, if a dynamic ellipticity of value H' is connected to an orbital frequency (for example, of precession or obliquity variations) of f', then, in the absence of resonance effects, the perturbation $\delta H/H'$ would yield a proportional perturbation in the associated frequency of $f'\delta H/H'$ (Laskar et al., 1993; Williams, 1994).

3. Results

Plate tectonics is driven by thermochemical convection within the Earth's mantle, a process that also leads to perturbations in the shape of the solid surface, core-mantle boundary, and gravitational field of the planet on a wide range of spatial scales. In the 1980s, global geophysical research focused on numerical and theoretical modeling of the process using constraints from satellite-derived estimates of Earth's long-wavelength gravity field (e.g., Richards and Hager, 1984; Ricard et al., 1984; Hager et al., 1985). These efforts combined tomographic models of seismic velocity variations in the mantle with experimental constraints from mineral physics on the mapping between these velocities and density (or, equivalently, buoyancy), with the goal of constraining the depth-dependent variation of mantle viscosity. While this approach provides invaluable insights on mantle dynamics, trade-offs between mantle buoyancy and viscosity render results subject to considerable uncertainty (Thoraval and Richards, 1997). Subsequent work therefore extended these studies to consider a wider range of present-day observations, including plate velocities, perturbations to surface topography, and excess ellipticity of the core-mantle boundary as inferred from the period of the Earth's free core nutation (e.g. Forte and Peltier, 1987; Lithgow-Bertelloni and Richards, 1998; Gurnis et al., 2000; Forte and Mitrovica, 2001; Simmons et al., 2006).

A number of studies have extended the present-day snapshot of mantle dynamics, the focus of the above analyses, to model the time history of the system. These analyses were generally based on "backward advection" of the governing field equations under the caveat that thermal diffusion is treated as negligible, since it is not temporally reversible in a unique sense and is not tractable due to numerical instabilities (Steinberger and O'Connell, 1997; Conrad and Gurnis, 2003; Moucha et al., 2008). A major limitation of this approach is that it produces transient behaviour within the thermal boundary layers (regions at the base and top of the convecting mantle, which are dominated by conductive heat transport), resulting in model simulations undergoing an initial jump prior to reaching steady-state; this jump contaminates the most recent period of model evolution. These issues are avoided in more sophisticated adjoint treatments that solve the full field equations in a forward sense and therefore rigorously incorporate thermal diffusion (e.g., Bunge et al., 2003; Ismail-Zadeh et al., 2004; Zhou and Liu, 2017; Li et al., 2017; Price and Davies, 2018; Ghelichkhan and Bunge, 2018).

Here, we adopt the adjoint methodology of Ghelichkhan and Bunge (2016) to track relative changes in the dynamical ellipticity driven by mantle convection over the past 50 Myr (Fig. 1A). Details of the calculation are provided in the Appendix A. Our simulation yields a perturbation in the magnitude of H of order 0.1% since 50 Ma, with an increase in dynamic flattening until 20 Ma, followed by a decrease of comparable magnitude in the subsequent 15 Myr (Fig. 1A). Our investigation of the evolving mantle heterogeneity in the adjoint model indicates that the increase in $\delta H/H$ from 50 Ma to 20 Ma is driven by an increase in the amplitude of long-wavelength density anomalies at the base of the upper mantle (the so-called transition zone) and the base of the lower mantle (i.e., above the fluid outer core). The subsequent change in trend reflects a progressive weakening of the transition zone signal after 20 Ma.

This variation in H is significantly smaller than predicted by a previous backward advection simulation (Forte and Mitrovica, 1997), and it has significant implications for the stability of Earth's precession and obliquity parameters. In particular, Laskar et al. (1993) has shown that if the dynamic flattening were perturbed downward by ~0.2% relative to the present day value, these parameters would experience a non-linear perturbation due to a passage through the $s_6-g_6+g_5$ resonance that is associated with perihelion of Jupiter and Saturn and the node of Saturn. We conclude that such a passage is unlikely to have occurred over the past 50 Myr (c.f. Forte and Mitrovica, 1997).

Next, we turn to variability in the dynamical ellipticity associated with ice age dynamics over the past 3 Myr. Over this period, the Earth was subject to glacial cycles of increasing magnitude, and an obliquity-paced periodicity of ~40 kyr until ~800 ka, followed by the so-called "Mid-Pleistocene transition" to cycles of period ~100 kyr (Lisiecki and Raymo, 2005). The last such cycle occurred from ~120–6 ka, with the Last Glacial Maximum reached at 26 ka, and it involved a mass flux equivalent to ~130 m of global average sea level change (Austermann et al., 2013). Our prediction of perturbations to the dynamical flattening (Fig. 1B) is generated using a theory of ice age dynamics that involves a gravitationally self-consistent treatment of sea level changes constrained to conserve the total (ice plus ocean) surface mass (Kendall et al., 2005) and it requires, on input, models for the radial profile of mantle viscosity and the full space-time geometry of ice mass changes. For the former, we adopt the same viscosity model used in our convection simulation to generate Fig. 1A, and for the latter, we use the ice history developed by Raymo et al. (2011).

Since the Earth is currently in an interglacial period, with high-latitude glaciation near a minimum, the mean perturbation of H relative to present day represents a reduction in the flattening of 0.12%. Over the same period, the convection-induced perturbation to H reaches 0.015% of the present-day value, and thus ice age dynamics dominate the perturbation in dynamical flattening across this 3 Myr time scale. The temporal variability in Fig. 1B reflects the history of forcing, with the above-noted transition in the period of cyclicity and a general change in the magnitude of variability at ~800 ka. Across the current interglacial (i.e., since 6 ka), the polar regions of the Earth are continuing to rebound from subsidence associated with 26–6 ka ice unloading, and this process is reflected in the gradual reduction in flattening that persists to the present day.

Finally, we turn our attention to recent variations in the dynamical flattening on decadal time scales. Fig. 1C shows the observed change in H across the satellite period, relative to 2012, derived from the results of Cheng et al. (2013). As discussed earlier, a change in the trend of the $\delta H/H_0$ time series, or equivalently J_2 from Eq. (5), took place around the year 1990. Prior to that date, the trend is dominated by the above-noted reduction in oblateness (and polar moment of inertia) since ~6 ka that is driven by ongoing effects of the ice age. This trend continues after 1990, but the onset of significant modern melting of ice sheets at that time contributes to an increase in oblateness (as ice melts near the poles and mass redistributes toward lower latitudes), resulting in a net signal that is characterized by a reduced trend (i.e., the magnitude of dH/dt and dJ_2/dt decreases).

In more quantitative terms, the rate of change in $\delta H/H_0$ prior to 1990 is -3.4×10^{-8} yr^{-1}, and it decreases in magnitude by approximately a factor of four to -0.8×10^{-8} yr^{-1} in the period 1990–2012. The ice age calculation of Fig. 1B predicts a contribution to the present-day rate of change of $\delta H/H_0$ of approximately -5.1×10^{-8} yr^{-1}, and correcting the two observed rates for this signal yields residuals of $\sim 1.7 \times 10^{-8}$ yr^{-1} and $\sim 4.3 \times 10^{-8}$ yr^{-1}, respectively. In the earlier period, 1976–1990, the remaining contributor to the signal is associated with melting of glaciers driven by global climate change. Mitrovica et al. (2015) estimated the rate of change of J_2 due to this glacier melting as $\sim 2.0 \pm 0.3 \times 10^{-11}$ yr^{-1}; this converts to a rate of change in $\delta H/H_0$ of $\sim 1.8 \times 10^{-8}$ yr^{-1}, a value which is in agreement with the (observed minus ice age-corrected) residual cited above ($\sim 1.7 \times 10^{-8}$ yr^{-1}). In the period after 1990, the larger ice age-corrected signal (4.3×10^{-8} yr^{-1}) reflects the onset of major melting from the polar ice sheets (Cox and Chao, 2002; Cheng et al., 2013). The best fit linear form across the full time series, i.e., 1976–2012, is characterized by a rate of change of $\delta H/H_0$ of $\sim -2.1 \times 10^{-8}$ yr^{-1}.

The calculations in Fig. 1, since they are based on Eq. (2), do not include the impact on the inertia tensor of a uniform, degree-0 deformation of the Earth. If we included this spatially uniform signal in the theory, Eq. (3) would be revised to

$$\delta H = \left[\frac{3}{2} - H\left(1 + \frac{\delta C_{(0,0)}}{\delta C_{(2,0)}}\right)\right] \frac{\delta C_{(2,0)}}{C}, \tag{8}$$

where the subscripts denote the spherical harmonic degree and order of the structure contributing to the inertia perturbation. In our calculations of perturbations in $\delta H/H$ due to ice mass changes (Fig. 1B), we include complementary sea level changes and the total mass of the surface load is conserved (i.e., it has no degree-0 component). The same must be true for the processes responsible for the observations that form the basis of Fig. 1C. Thus, in these cases, there is no degree-0 deformation, $\delta C_{(0,0)} = 0$, and the above expression collapses to that in Eq. (3). While our calculations of the perturbation to $\delta H/H$ driven by mantle convection adopt a compressible flow model, any changes in the volume of the Earth are negligible. However, these calculations do not account for secular cooling and thermal contraction of the Earth. Estimates of this latter process suggest that the reduction in Earth radius over the past 50 Myr due to thermal contraction has been ~80 m (Tsuchiya et al., 2013). Using this value and the results in Fig. 1A yields an estimate of $\delta C_{(0,0)}/\delta C_{(2,0)} \sim 5$, and therefore $H(1 + \delta C_{(0,0)}/\delta C_{(2,0)}) \sim 6H$. This value is of order 1% of the leading term of $\frac{3}{2}$ in Eq. (8), and neglecting it in adopting Eq. (4) remains justified.

The results in Fig. 1 do not include the impact on the dynamical flattening of an additional process mentioned in the introductory section, namely, tidal dissipation. The present level of tidal dissipation is slowing the Earth's rotation at a rate of $(d\Omega/dt)/\Omega = 8.8 \times 10^{-18}$ s^{-1} (e.g. Quinn et al., 1991) and the dynamical flattening will be approximately proportional to Ω^2. While the variation of tidal dissipation over time is uncertain, any effort to estimate the total change in dynamical flattening from all geophysical processes must include this contribution.

4. Final remarks

The dynamical flattening of the Earth, a parameter associated with the precession constant, plays an important role in a wide range of applications in astronomy, geodesy and geophysics, including astronomical observations of nutations, investigations of the stability of the orbital elements (precession, obliquity) controlling Milankovitch forcing of ice age climate, and the evolution of the Earth-Moon-Sun system over billion-year time scales. Burša et al. (2008) highlighted the importance of recognizing the time dependence in the precession constant within astronomical analyses. However, they suggested that the variation in H could be captured by a constant rate term computed by fitting a linear form through a satellite time series of J_2 extending from 1979 to 2002 – they derived a value for dH/dt of -8.45×10^{-11} yr^{-1}, or equivalently a rate of change of $\delta H/H_0$ of $\sim 2.6 \times 10^{-8}$ yr^{-1} – and advocated that the rate be adopted as a fundamental astro-geodetic parameter. In contrast to this view, we have shown in Fig. 1 that time dependence of the dynamic ellipticity is highly non-linear, even when considering only the last 40 years of satellite-based measurements (Fig. 1C). The full complexity of the time series of $\delta H/H_0$ in Fig. 1 reflects the suite of geophysical processes that perturb the Earth's flattening, including mantle convection, ice age dynamics, and modern global climate change.

Declaration of Competing Interest

None.

Acknowledgements

SG is indebted to D.R. Davies for guidance and support. We acknowledge funding and support from Harvard University (JJF, JXM), National Aeronautics and Space Administration grant NNX17AE17G (MJH, JXM), the American Chemical Society Petroleum Research Fund grant 59062-DNI8 (MJH), Imperial College Research Fellowshipscheme and the Schmidt Science Fellows Program (FDR).

Appendix A

Time-evolution in our adjoint treatment (Ghelichkhan and Bunge, 2016) is constrained by assimilating a history of plate motions (Young et al., 2019), and the initial buoyancy field (i.e., at 50 Ma) is iteratively optimized through comparison of the final, present-day buoyancy field predicted by the flow model with the buoyancy field inferred from seismic tomography. This procedure typically converges after 12–15 iterations.

Two other fields need to be prescribed in this procedure, the radial viscosity structure used in the flow calculation and the present-day mantle buoyancy field to which the prediction of the flow model at the present day is compared. We consider each, in turn. All other material parameters and boundary conditions are adopted from Colli et al. (2018).

We use a radial viscosity profile derived from a joint inversion of data related to mantle convection and ice age dynamics (Mitrovica and Forte, 2004). The viscosity model, which we also adopt in the ice age calculations described in the main text, is characterized by a three order of magnitude increase in viscosity from the shallow mantle beneath the lithosphere (10^{20} Pa s) to 2000 km depth (10^{23} Pa s), followed by a reduction of comparable magnitude toward the core-mantle-boundary.

To construct the present-day mantle buoyancy field, we use lower mantle shear wave velocities from the recent tomography model `LLNL-G3D` (Simmons et al., 2012). Upper mantle velocity structure is prescribed from the higher resolution surface wave tomography model `SL2013sv` (Schaeffer and Lebedev, 2013), smoothly blended into the deeper mantle model over the depth range 250–350 km. To convert seismic velocities into density, we first calculate anharmonic velocities and densities as a function of pressure and temperature for a pyrolitic mantle composition using the thermodynamic database of Stixrude and Lithgow-Bertelloni (2011) and the `Perple_X` Gibbs free-energy minimisation software (Connolly, 2005). Next, anharmonic velocities are corrected for anelasticity using the `Q5` attenuation model of Cammarano et al. (2003), adopting the solidus of Hirschmann (2000) in the upper ~250 km and Andrault et al. (2011) in the deeper mantle. Tomographically inferred velocity variations as a function of depth are then used to query the resulting lookup table and extract corresponding values of density. To prevent the continental lithosphere from actively participating in convection, densities within the lithosphere are set to the radial average using the lithosphere-asthenosphere boundary map of Hoggard et al. (2020).

Once the temporal evolution of the mantle flow field has been successfully reconstructed, we calculate the time history of dynamic ellipticity, H. For this purpose, we solve the governing, coupled system of Stokes and Poisson's equations using an instantaneous flow methodology that includes the effects of self-gravitation and compressiblity and assumes a free-slip (no tangential stress) boundary condition (Corrieu et al., 1995).

References

Andrault, D., Bolfan-Casanova, N., Nigro, G.L., Bouhifd, M.A., Garbarino, G., Mezouar, M., 2011. Solidus and liquidus profiles of chondritic mantle: implication for melting of the Earth across its history. Earth Planet. Sci. Lett. 304, 251–259.

Austermann, J., Mitrovica, J.X., Latychev, K., Milne, G.A., 2013. Barbados-based estimate of ice volume at Last Glacial Maximum affected by subducted plate. Nat. Geosci. 6, 553–557.

Bunge, H.-P., Hagelberg, C.R., Travis, B.J., 2003. Mantle circulation models with variational data assimilation: inferring past mantle flow and structure from plate motion histories and seismic tomography. Geophys. J. Int. 152, 280–301.

Burša, M., Groten, E., Šíma, Z., 2008. Steady change in flattening of the earth: the precession constant and its long-term variation. Astron. J. 135, 1021–1023.

Cammarano, F., Goes, S., Vacher, P., Giardini, D., 2003. Inferring upper-mantle temperatures from seismic velocities. Phys. Earth Planet. Inter. 138, 197–222.

Chambat, F., Ricard, Y., Valette, B., 2010. Flattening of the Earth: further from hydrostaticity than previously estimated. Geophys. J. Int. 183, 727–732.

Chao, B.F., 2017. On rotational normal modes of the earth: resonance, excitation, convolution, deconvolution and all that. Geodesy and Geodynamics 8, 371–376.

Cheng, M., Tapley, B.D., Ries, J.C., 2013. Deceleration in the Earth's oblateness. Journal of Geophysical Research: Solid Earth 118, 740–747.

Colli, L., Ghelichkhan, S., Bunge, H.P., Oeser, J., 2018. Retrodictions of mid Paleogene mantle flow and dynamic topography in the Atlantic region from compressible high resolution adjoint mantle convection models: sensitivity to deep mantle viscosity and tomographic input model. Gondwana Res. 53, 252–272.

Connolly, J.A., 2005. Computation of phase equilibria by linear programming: a tool for geodynamic modeling and its application to subduction zone decarbonation. Earth Planet. Sci. Lett. 236, 524–541.

Conrad, C.P., Gurnis, M., 2003. Seismic tomography, surface uplift, and the breakup of Gondwanaland: integrating mantle convection backwards in time, *Geochemistry, Geophysics*. Geosystems 4 (3).

Corrieu, V., Thoraval, C., Ricard, Y., 1995. Mantle dynamics and geoid green functions. Geophys. J. Int. 120, 516–523.

Cox, C.M., Chao, B.F., 2002. Detection of a large-scale mass redistribution in the terrestrial system since 1998. Science 297, 831–833.

Dehant, V., Capitaine, N., 1996. On the precession constant: values and constraints on the dynamical ellipticity, Link with Oppolzer terms and tilt-over-mode. Celestial Mechanics and Dynamical Astronomy 65, 439–458.

Forte, A.M., Mitrovica, J.X., 1997. A resonance in the Earth's obliquity and precession over the past 20 Myr driven by mantle convection. Nature 390, 676–680.

Forte, A.M., Mitrovica, J.X., 2001. Deep-mantle high-viscosity flow and thermochemical structure inferred from seismic and geodynamic data. Nature 410, 1049–1056.

Forte, A.M., Peltier, W.R., 1987. Plate tectonics and aspherical Earth structure: the importance of poloidal- toroidal coupling. J. Geophys. Res. 92 (B5), 3645–3679.

Ghelichkhan, S., Bunge, H.-P., 2016. The compressible adjoint equations in geodynamics: derivation and numerical assessment. International Journal on Geomathematics 7, 1–30.

Ghelichkhan, S., Bunge, H.P., 2018. The adjoint equations for thermochemical compressible mantle convection: derivation and verification by twin experiments. Proceedings of the Royal Society A 474 (20180329).

Gurnis, M., Mitrovica, J.X., Ritsema, J., van Heijst, H.-J., 2000. Constraining mantle density structure using geological evidence of surface uplift rates: the case of the African Superplume. Geochemistry, Geophysics, Geosystems 1 (1020).

Hager, B.H., Clayton, R.W., Richards, M.A., 1985. Lower mantle heterogeneity, dynamic topography and the geoid. Nature 313, 541–545.

Hansen, K.S., 1982. Secular effects of oceanic tidal dissipation on the Moon's orbit and the Earth's rotation. Rev. Geophys. 20 (3), 457–480.

Hirschmann, M.M., 2000. Mantle solidus: experimental constraints and the effects of peridotite composition. Geochemistry Geophysics Geosystems 1 (10).

Hoggard, M.J., Czarnota, K., Richards, F.D., Huston, D.L., Jaques, A.L., Ghelichkhan, S., 2020. Global distribution of sediment-hosted metals conrolled by craton edge stability. Nat. Geosci. 13, 504–510.

Ismail-Zadeh, A., Schubert, G., Tsepelev, I., Korotkii, A., 2004. Inverse problem of thermal convection: numerical approach and application to mantle plume restoration. Phys. Earth Planet. Inter. 145, 99–114.

Kaula, W.M., Harris, A.W., 1975. Dynamics of lunar origin and orbital evolution. Rev. Geophys. Space Phys. 13 (2), 363–371.

Kendall, R.A., Mitrovica, J.X., Milne, G.A., 2005. On post-glacial sea level - II. Numerical formulation and comparative results on spherically symmetric models. Geophysical Journal International 161, 679–706.

Laskar, J., Joutel, F., Boudin, F., 1993. Orbital, precessional, and insolation quantities for the earth from −20 Myr to +10 Myr. Astron. Astrophys. 270, 522–533.

Li, D., Gurnis, M., Stadler, G., 2017. Towards adjoint-based inversion of time-dependent mantle convection with nonlinear viscosity. Geophys. J. Int. 209, 86–105.

Lisiecki, L.E., Raymo, M.E., 2005. A Pliocene-Pleistocene stack of 57 globally distributed benthic δ18O records. Paleoceanography 20 (PA1003).

Lithgow-Bertelloni, C., Richards, M.A., 1998. The dynamics of Cenozoic and Mesozoic plate motions. Rev. Geophys. 36 (1), 27–78.

Lourens, L.J., Wehausen, R., Brumsack, H.J., 2001. Geological constraints on tidal dissipation and dynamical ellipticity of the earth over the past three million years. Nature 409, 1029–1033.

Mitrovica, J.X., Forte, A.M., 2004. A new inference of mantle viscosity based upon joint inversion of convection and glacial isostatic adjustment data. Earth Planet. Sci. Lett. 225, 177–189.

Mitrovica, J.X., Forte, A.M., Pan, R., 1997. Glaciation-induced variations in the Earth's precession frequency, obliquity and insolation over the last 2.6 Ma. Geophys. J. Int. 128, 270–284.

Mitrovica, J.X., Hay, C.C., Morrow, E., Kopp, R.E., Dumberry, M., Stanley, S., 2015. Reconciling past changes in Earth's rotation with 20th century global sea-level rise: resolving Munk's enigma. Sci. Adv. 1 (e1500679).

Morrow, E., Mitrovica, J.X., Forte, A.M., Glišović, P., Huybers, P., 2012. An enigma in estimates of the Earth's dynamic ellipticity. Geophys. J. Int. 191, 1129–1134.

Moucha, R., Forte, A.M., Mitrovica, J.X., Rowley, D.B., Quéré, S., Simmons, N.A., Grand, S.P., 2008. Dynamic topography and long-term sea-level variations: there is no such thing as a stable continental platform. Earth Planet. Sci. Lett. 271, 101–108.

Nakiboglu, S.M., 1982. Hydrostatic theory of the earth and its mechanical implications. Phys. Earth Planet. Inter. 28, 302–311.

Pälike, H., Shackleton, N.J., 2000. Constraints on astronomical parameters from the geological record for the last 25 Myr. Earth Planet. Sci. Lett. 182, 1–14.

Price, M.G., Davies, J.H., 2018. Profiling the robustness, efficiency and limits of the forward-adjoint method for 3-D mantle convection modelling. Geophys. J. Int. 212, 1450–1462.

Quinn, T.R., Tremaine, S., Duncan, M., 1991. A three million year integration of the Earth's orbit. Astron. J. 101 (6), 2287–2305.

Raymo, M.E., Mitrovica, J.X., O'Leary, M.J., Deconto, R.M., Hearty, P.J., 2011. Departures from eustasy in Pliocene Sea-level records. Nat. Geosci. 4, 328–332.

Ricard, Y., Fleitout, L., Froidevaux, C., 1984. Geoid heights and lithospheric stresses for a dynamic earth. Ann. Geophys. 2, 267–286.

Richards, M.A., Hager, B.H., 1984. Geoid anomalies in a dynamic Earth. J. Geophys. Res. 89 (B7), 5987–6002.

Rochester, M.G., Smylie, D.E., 1974. On changes in the trace of the Earth's inertia tensor. J. Geophys. Res. 79 (32), 4948–4951.

Roy, K., Peltier, W.R., 2011. GRACE era secular trends in Earth rotation parameters: a global scale impact of the global warming process? Geophys. Res. Lett. 38 (L10306).

Schaeffer, A.J., Lebedev, S., 2013. Global shear speed structure of the upper mantle and transition zone. Geophys. J. Int. 194, 417–449.

Simmons, N.A., Forte, A.M., Grand, S.P., 2006. Constraining mantle flow with seismic and geodynamic data: a joint approach. Earth Planet. Sci. Lett. 246, 109–124.

Simmons, N.A., Myers, S.C., Johannesson, G., Matzel, E., 2012. LLNL-G3Dv3: global P wave tomography model for improved regional and teleseismic travel time prediction. Journal of Geophysical Research: Solid Earth 117 (B10302).

Steinberger, B., O'Connell, R.J., 1997. Changes of the Earth's rotation axis owing to advection of mantle density heterogeneities. Nature 387, 169–173.

Stephenson, F.R., 2003. Historical eclipses and Earth's rotation. Astron. Geophys. 44 (2), 22–27.

Stephenson, F.R., Morrison, L.V., 1984. Long-term changes in the rotation of the earth: 700 B.C. to a.D. 1980. Philos. Trans. R. Soc. Lond. A 313, 47–70.

Stephenson, F.R., Morrison, L.V., 1995. Long-term fluctuations in the Earth's rotation: 700 BC to AD 1990. Philos. Trans. R. Soc. Lond. A 351, 165–202.

Stixrude, L., Lithgow-Bertelloni, C., 2011. Thermodynamics of mantle minerals – II. Phase equilibria. Geophysical Journal International 184, 1180–1213.

Thoraval, C., Richards, M.A., 1997. The geoid constraint in global geodynamics: viscosity structure, mantle heterogeneity models and boundary conditions. Geophys. J. Int. 131, 1–8.

Tsuchiya, T., Kawai, K., Maruyama, S., 2013. Expanding-contracting Earth. Geosci. Front. 4, 341–347.

Wahr, J.M., 1981. Body tides on an elliptical, rotating, elastic and oceanless earth. Geophys. J. R. Astron. Soc. 64, 677–703.

Williams, J.G., 1994. Contributions to the Earth's obliquity rate, precession, and nutation. Astron. J. 108, 711–724.

Williams, G.E., 1997. Precambrian length of day and the validity of tidal rhythmite paleotidal values. Geophys. Res. Lett. 24 (4), 421–424.

Young, A., Flament, N., Maloney, K., Williams, S., Matthews, K., Zahirovic, S., Müller, R. D., 2019. Global kinematics of tectonic plates and subduction zones since the late Paleozoic Era. Geosci. Front. 10, 989–1013.

Zhou, Q., Liu, L., 2017. A hybrid approach to data assimilation for reconstructing the evolution of mantle dynamics. Geochem. Geophys. Geosyst. 18, 3854–3868.

Siavash Ghelichkhan[a,*], Jocelyn J. Fuentes[b], Mark J. Hoggard[b,c], Fred D. Richards[d], Jerry X. Mitrovica[b]

[a] *Research School of Earth Sciences, Australian National University, 142 Mills Rd, Acton ACT 200, Australia*

[b] *Department of Earth & Planetary Sciences, Harvard University, 20 Oxford Street, Cambridge, MA 02138, USA*

[c] *Lamont-Doherty Earth Observatory, Columbia University, 61 Rte 9W, Palisades, NY 10964, USA*

[d] *Royal School of Mines, Imperial College London, South Kensington Campus, London SW7 2AZ, UK*

E-mail addresses: siavash.ghelichkhan@anu.edu.au (S. Ghelichkhan), jxm@eps.harvard.edu (J.X. Mitrovica).

[*] Corresponding author.